

Effects of neutron and gamma radiation on lithium-ion batteries

Jie Qiu^{a,1}, Dandan He^{a,1}, Mingzhai Sun^b, Shimeng Li^c, Cun Wen^d, Jason Hattract-Simpers^d, Yuan F. Zheng^c, Lei Cao^{a,*}

^a Nuclear Engineering Program, Department of Mechanical and Aerospace, The Ohio State University, Columbus, OH 43210, USA

^b Davis Heart and Lung Research Institute, The Ohio State University, Columbus, OH 43210, USA

^c Department of Electrical and Computer Engineering, The Ohio State University, Columbus, OH 43210, USA

^d Department of Chemical Engineering, University of South Carolina, Columbia, SC 29208, USA

ARTICLE INFO

Article history:

Received 24 October 2014

Received in revised form 18 December 2014

Accepted 18 December 2014

Available online 12 January 2015

Keywords:

Li-ion battery

Neutron radiation

Gamma radiation

Atomic force microscopy

Capacity loss

ABSTRACT

Radiation induced deterioration in the performance of lithium-ion (Li-ion) batteries can result in functional failures of electronic devices in modern electronic systems. The stability of the Li-ion battery under a radiation environment is of crucial importance. In this work, the surface morphology of the cathode material of a commercial Li-ion battery before and after neutron and gamma ray irradiation was characterized by atomic force microscopy (AFM). We found growth in the particle size of the cathode material in the range of 36–45% as a result of the irradiation. In addition, X-ray diffraction (XRD) patterns revealed a disordering of the crystal structure occurring in the post-irradiation sample. All of these led to a 8.4% capacity loss of the battery for the maximum received irradiation dose (2.744 Mrad) at post-irradiation. The effects of the radiation on the Li-ion battery are discussed in this paper.

© 2014 Elsevier B.V. All rights reserved.

1. Introduction

As one of the most popular rechargeable batteries, Li-ion batteries (LIB) have several unique properties, such as a high energy density, large specific capacity, and a lightweight structure [1]. In addition to their wide applications in household appliances, modern electronic gadgets, electric vehicles, LIBs also have emerging applications in systems for security purposes, such as rescuing and sampling equipment in nuclear environments. For example, in the 2011 Fukushima nuclear accident, robots were deployed to conduct sampling, recovery, and rescue missions in the radiation-intense environments, but they quickly failed [2]. Considering that LIBs are the power source for such robots, understanding the effect of radiation on their performance is critically important for their reliable application in harsh radiation environments.

Prior research, although limited in this area, has indicated that LIB performance is affected by irradiation, with microstructural changes in the electrode materials playing a chief role in battery capacity fade. While NASA reported a certain level of radiation

resistance in commercial LIBs to gamma radiation exposure [3], Ding et al. demonstrated that radiation results in defects and disorder in the crystal lattice of the LiCoO₂ cathode material, subsequently influencing the capacity of the battery [4]. To the best of our knowledge, no work has been done to link the relationship between the cathode material's microstructure and the LIB capacity change after neutron or gamma radiation. In this paper, we focus on the characterization of the LIB cathode material microstructure before and after irradiation by atomic force microscopy (AFM) and X-ray diffraction (XRD). Furthermore, the degradation of the batteries at the cell level, such as the post-irradiation capacity loss, is also reported. Neutron fluence levels ranging from 10¹² to 10¹⁵ n/cm² and gamma ray dose levels from 0.098 to 2.744 Mrad were applied to the LIBs.

2. Materials and methods

2.1. Samples

Commercially available LIBs, manufactured by Kokam Co., Ltd., were used in this study. These LIBs are of the punch format type. An illustration of its components are shown in Fig. 1. The cathode material is LiCoO₂, attached to an aluminum current collector, and the anode material is graphite with a copper current collector, the electrolyte here is LiPF₆ EC:EMC.

Abbreviations: AFM, atomic force microscopy; XRD, X-ray diffraction; LIB, lithium-ion battery; LiCoO₂, lithium cobalt oxide.

* Corresponding author.

E-mail address: cao.152@osu.edu (L. Cao).

¹ The first and second author contribute equally to this work.

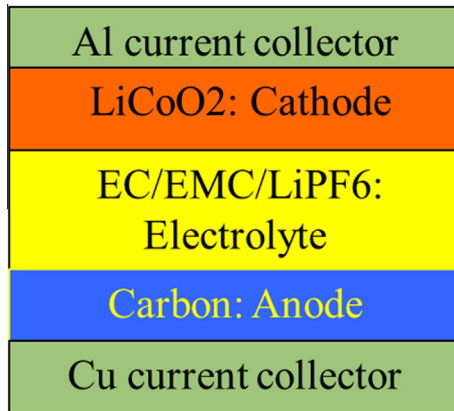


Fig. 1. A schematic of the components for the LIBs used in this study.

Table 1
Neutron fluence and neutron flux for each sample.

Sample	Fast neutron fluence (n/cm ²)/flux (n/cm ² /s)	Thermal neutron fluence (n/cm ²)/flux (n/cm ² /s)	Total neutron fluence (n/cm ²)
1	$2.0 \times 10^{11}/5.0 \times 10^9$	$8.0 \times 10^{11}/2.0 \times 10^{10}$	1.0×10^{12}
2	$2.0 \times 10^{12}/1.0 \times 10^{10}$	$8.0 \times 10^{12}/4.0 \times 10^{10}$	1.0×10^{13}
3	$2.0 \times 10^{13}/1.0 \times 10^{11}$	$8.0 \times 10^{13}/4.0 \times 10^{11}$	1.0×10^{14}
4	$2.0 \times 10^{14}/4.5 \times 10^{11}$	$8.0 \times 10^{14}/1.8 \times 10^{12}$	1.0×10^{15}
5	$1.0 \times 10^{12}/5.1 \times 10^9$		1.0×10^{12}
6	$1.0 \times 10^{13}/1.0 \times 10^{11}$		1.0×10^{13}
7	$1.0 \times 10^{14}/4.6 \times 10^{11}$		1.0×10^{14}
8	$1.0 \times 10^{15}/4.6 \times 10^{11}$		1.0×10^{15}

Eight cathode samples taken from pristine batteries were irradiated at the “rabbit” at the Ohio State University Research Reactor (OSURR). Fast plus thermal neutrons (with an energy less than 0.4 eV and a peak at 0.0253 eV) and fast neutrons only (with an average energy of 1.98 MeV and a more probable energy of 0.73 MeV) were applied to the cathode samples. The detailed irradiation conditions are listed in Table 1. A cadmium button was used to filter out the thermal neutron component to obtain the fast neutron only irradiation environment, since the cadmium thickness (1 mm) is essentially opaque to thermal neutrons. The sample without the cadmium covering will receive a mixture of thermal and fast neutron fluences.

The gamma ray irradiation was performed at the Ohio State University Nuclear Reactor Lab (OSUNRL) using a cobalt-60 (Co-60) isotope source that is housed in the bottom of a water pool. The Co-60 source, which has a dose rate of 39.2 kRad/h and two major cascade gamma rays at 1.173 and 1.332 MeV, was evenly spread around an aluminum tube in the water. The aluminum tube contains a movable platform that can raise or lower the irradiator.

2.2. Atomic force microscopy measurements

Since AFM is widely used to image the surface topography of a sample with extremely high resolution, the surface features of the cathodes at pre- and post-irradiation were characterized, obtaining the particle height profiles for insights on the irradiation induced size change. The AFM measurements were performed on a Bioscope II (Veeco), operating under contact mode with gold-coated AFM probes (MSCT; Veeco). Images of all samples were collected over a scan area of $1 \times 1 \mu\text{m}$, taken in air at room temperature. The Nanoscope software was used to analyze the obtained images.

2.3. XRD characterization

The XRD data were collected with a Miniflex II X-ray diffractometer (Rigaku) using a sealed Cu X-ray tube (Cu K α X-rays of 0.1541837 nm) operating at 30 kV and 15 mA. Measurements of each sample were performed in the 2θ range from 10 to 90° with a 2°/min scanning speed and a 0.02° scanning step size.

2.4. Capability measurement pre- and post-gamma irradiation

A programmable DC electronic load B&K 8500 (BK Precision) is used to obtain the discharge curve of batteries in our experiment. The B&K 8500 essentially works as an electric load consuming the energy of a power supply which is connected to the input of the instrument. It can work under the constant current mode, which discharges the battery at a constant but adjustable current. In our experiments, the constant mode is used and the fully charged voltage is set to 4.17–4.18 V for the batteries. Initially the fully charged battery samples were connected to the input of the B&K 8500. The battery is then discharged according to the rate set. The B&K 8500 records the voltage of the input while it discharges the battery. A discharge curve showing the voltage as a function of time is obtained. The first test is on un-irradiated batteries, and the obtained curves serve as the reference. The batteries were then fully recharged again before being exposed to the Co-60 source for 2.5, 18, and 70 h, rendering a total dosage of 0.098, 0.706, and 2.744 Mrad, respectively. The batteries went through the discharging tests one by one, post-irradiation, to obtain their respective discharge curves. Those discharge curves are compared with the reference discharge curves to evaluate how the radiation affects the performance of the ion-batteries.

3. Results and discussion

The AFM height images, *i.e.*, the grain size at the Z-scale, of the cathode samples with different neutron fluences (10^{12} – 10^{15} are shown in Fig. 2(a)–(c)). In order to quantify the grain size variation at post-irradiation, the conjugate diameter of each particle in every AFM image was measured. While the size change is not visually intuitive in the AFM images (Fig. 2), the statistical analysis of the particle size distribution, as shown in Fig. 3, reveals that the radii of the LiCoO₂ particles have increased after neutron irradiation. The particle size distribution in the AFM images at each level of neutron irradiation is displayed in a box plot (Fig. 3(a) and (b)), where the minimum, maximum, four quartiles (minimum point to the bottom line of the box as the first quartile, maximum point to the upper line of the box as the fourth quartile), and the median level (middle line of the box) of the data set are all displayed.

It can be seen from Fig. 3 that the increase in grain size was small when the neutron fluence was less than 10^{13} n/cm², regardless if the fast plus thermal or only fast neutron irradiation was used. However, the grain size has a greater degree of change at the higher fluence, for example, the mean value increases from 73.4 at pre-irradiation to 82.1 at 10^{13} n/cm² and quickly rises to 100.4 at 10^{14} n/cm² neutron fluence.

Derived from the AFM height images, the root-mean-square roughness (*Rq*) was quantified and plotted in Fig. 4, which again reveals a correlation to neutron fluence. The conclusion that the particle size increased with higher neutron fluence is reasonably corroborated by Fig. 4, as larger grains are inherently rougher due to the increased height differences (*Z* range) at their boundaries. It appears that the trend of increasing particle size became more evident under the fast neutron irradiation compared to the fast plus thermal neutron irradiation, as shown in Figs. 3 and 4.

Download English Version:

<https://daneshyari.com/en/article/1680627>

Download Persian Version:

<https://daneshyari.com/article/1680627>

[Daneshyari.com](https://daneshyari.com)